AADE-18-FTCE-SPP-04

An Experimental Study on the Impact of Total Dissolved Solids and Total Suspended Solids on Friction Reducers for the Reuse of Flowback

M. H. Gipson and T. C. Nguyen, New Mexico Institute of Mining and Technology; H. Wiggins and E. Vinson, Chemplex Solvay Group

Abstract

The objective of this study is to experimentally look at the impact of total dissolved solids (TDS) and total suspended solids (TSS) on friction reducers (FR) for the reuse of flowback. Hydraulic tests were performed on three different commercial FRs: anionic FR-A, anionic FR-B, and cationic FR-C to observe their performance. FRs were varied in concentration and allowed to hydrate. Sodium chloride and calcium chloride were added to simulate TDS and calcium carbonate was added to simulate TSS found in flowback. Rheological tests were performed to observe the effects salinity had on the properties of slickwater. Hydraulic tests show after TDS were added to FR-A and FR-C solutions, an increase in friction reduction by 20% at 300,000 Reynolds number when compared to fresh water hydrated solutions at the same Reynolds number. This is because the fluids containing TDS have less apparent viscosity due to the salt thinning the solution, allowing the turbulent drag reduction component to have an increased effect on percent friction reduction (%FR) and the viscosity to have less of effect. FR-B does not benefit from the thinning effect of the salinity due to its rheology. When TSS were introduced to the FR solutions there was minimal effect on performance. The method used in this study for mixing flowback into fracturing fluids could improve the performance of some FRs in slickwater jobs and thus reducing the cost on well stimulation and disposal of flowback.

Introduction and Literature Review

Hydraulic fracturing is used to stimulate wells for increased production in hydrocarbon wells using primarily fresh water based fluids mixed with friction reducers for assistance in reducing pipe friction. The amount of fresh water used can be between 1-6 million gallons per well (Oraki, 2016). In many areas where oil and gas operations are using hydraulic fracturing, water is a scarce and expensive commodity (Barnes, 2015). After stimulation jobs, wells are flowed back, and some of the water initially injected returns to the surface as FB. Produced water is similar to FB water, however it comes out of wells during production life of the well; in this study it will also be referred to as flowback. FB contains mostly water and salts dissolved in solution from the formation, the concentration is referred to as TDS. There are also small suspended solids that come out from the formation and these concentrations are referred to as TSS. **Table 1** shows what popular plays around the US have for FB composition and return. Few chemicals from the hydraulic fracturing job can be found dissolved in solution, the concentration of these are very low and are not looked at in this experiment. The effects of TDS and TSS have known affects to slickwater fracturing fluids (Mantell, 2011). Experimentally looking at the how varying concentrations of FR, TDS, and TSS interact together help in understanding how to best use FB for the best performance. Disposing FB has become increasingly more difficult for operators due to regulations and high costs of disposal. The reuse of FB could reduce the costs of fresh water usage and lower disposal costs for operators.

Table 1: Main Producing Plays in United States (Paktinat et al., 2011)

Producing Area	TDS (ppm)	% FB
Bakken	150k – 300k	15 – 40
Eagle Ford	15k – 55k	<15
Permian Basin	20k – 300k	20 – 40
Marcellus	20k – 100k	10 – 40
Denver – Julesburg	20k – 65k	15 – 30

The Environmental Protection Agency (EPA) estimates that between 70 and 140 billion gallons of water is needed annually for hydraulic fracturing treatments in the US alone (U.S. EPA, 2016). For areas like the Eagle Ford, Permian, and Barnett integrated water management solutions and implemented operational practices must be put in place. This is required to continue supporting the completion operations due to their surface area of the play being impacted by drought conditions (13, Oraki, 2016). In these areas reusing FB in large quantities over fresh water could eliminate many stresses put on fresh water reserves.

Friction Reducers

Synthetic friction reducers primarily applied to stimulation are based on acrylamide copolymers. This high molecular weight polyacrylamide based polymer (PAM) is the most important component in slickwater and the common friction reducer used in the industry. The structure and charge of PAM can often be manipulated for an ideal performance level, dependent on the specific application; they can range from anionic, cationic, nonionic, and amphoteric. PAM can be highly effective in reducing horsepower required to move large volumes of fluid at high rates after being injected into the fluid “on the fly”. The amount of FR used in slickwater fracture treatments is usually 0.17% or less of the total fluid used (King, 2012). Typical concentrations added to slickwater treatments range from 0.5-1.75gpt. The mechanism that allows friction reducers to give benefits during turbulent flow has been highly studied and explained (Landahl, 1977), (Lumley, 1973), (Virk, 1975) through turbulent drag reduction. Lumley (1973) explained it to be due to the turbulent drag reduction and is related to the Prandtl Mixing theory. The Prandtl mixing theory for Newtonian flow regimes splits the cross sectional velocity profile into two layers: a viscous sub-layer, that exhibits laminar behavior, near the pipe wall and an inertial layer to the center of the pipe. In the viscous sub-layer, the eddies fall into a dissipation range, and the shear stress is linearly proportional to the velocity gradient or shear rate. The fluctuating velocities in the radial direction are small and not impairing flow while the axial velocities are at a maximum. The pressure losses in this flow region are considerably smaller than that of the inertial layer. The inertial layer has turbulent flow and the stresses are proportional to the mean velocity gradient. As the Reynolds number (Re) increases, the fluctuating radial velocities get larger, causing more energy to be lost. The inertial layer and the viscous sublayer locations can be seen in **fig. 1a.** With the presence of PAM, the long chain molecules are stretched by the large radial velocities creating a non-Newtonian regime that creates a drag reducing layer. This layer is found in-between the viscous sub-layer and the inertial layer, it is called the elastic sublayer. Diamond et al. (1992) describes fluctuating radial velocities in the buffer layer as smaller than inertial layer, but the fluctuating axial velocities actually increase. This essentially means that the radial velocities have transferred into slipping axial velocities giving the fluid more energy momentum in the flowing direction. **Fig. 1b** shows a visual of the layers relative to the pipe wall.

An important component of FRs when looking at performance is their inversion time. This is defined as the time required for the polymer to unfold and achieve its full drag reduction potential. A polymer requires that it reaches its maximum inversion time in the aqueous solution prior to the fracturing fluid entering the wellhead to optimize friction reduction. Most friction reducers designed for fresh water applications invert slowly in high brine waters. Making this difficult for optimal performance during slickwater jobs when using water that contains TDS.

Friction reducer performance in the lab is measured by a pressure drop over a standard length of pipe at a constant flow rate. A flow loop is the most common way to measure that pressure drop. Since there are many flow loop designs and variance between researchers the comparison of absolute friction reduction can be difficult. However, measuring the performance between friction reducers in the same loop and performance rankings between other loops would be expected to be consistent (Paktinat et al., 2011).

This study began its experiments by looking at the rheology of three separate commercially used FRs (descriptions of each FR can be found in the Appendix A) under laminar flow with a rotational viscometer. The rotational viscometer measures shear stresses of a fluid at different shear rates. These tests were conducted at varying concentrations of the three FRs and allowed to hydrate. Then adding varying concentrations of sodium chloride (NaCl) and calcium chloride ($CaCl_2$) to simulate TDS from FB. Calcium carbonate was also added to simulate suspended solids in FB.

The supplementary portion of experiments uses New Mexico Institute of Mining and Technology’s Hydraulic Testing Facility (HTF) to conduct hydraulic testing simulating turbulent pumping conditions found in the field. The same solutions used in rheology testing were pumped through a flow loop with instruments measuring flowrate, temperature, and pressure. The differential pressure of each fluid batch was measured at different flow rates to build a profile of the performance across a range.

Data collected throughout these two experiments were analyzed. The rheological properties are required to analyze turbulent flow conditions from the HTF. The combination of these results will tell which FR would perform best under the tested concentrations of TDS and TSS.

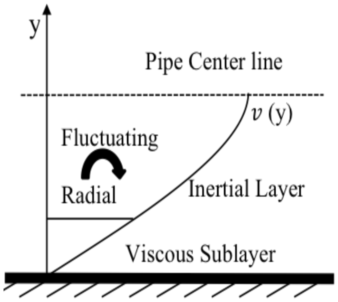

Fig.1a: Prandtl Mixing Length Theory Newtonian conditions

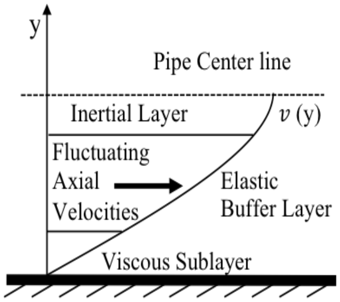

Fig. 1b: Prandtl Mixing length Theory non-Newtonian

Objective

The objective of the research is to experimentally look at the impact of TDS and TSS on three commercially used FRs for the reuse of FB. This includes determining the rheology effects of TDS and TSS on the FRs, and the performance of %FR under these conditions.

Table 2: Experimental Test Matrix

FR (pptg) & (g/L)	NaCl (g/L)	$CaCl_2$ (g/L)	NaCl (g/L)	$CaCl_2$ (g/L)	NaCl (g/L)	$CaCl_2$ (g/L)	NaCl (g/L)	$CaCl_2$ (g/L)	NaCl (g/L)	$CaCl_2$ (g/L)	TSS (ppm)
4ppgt & 0.478g/L	0	0	18	2	45	5	90	10	180	20	0-5k
6pptg &0.718g/L	0	0	18	2	45	5	90	10	180	20	
8pptg & 0.957g/L	0	0	18	2	45	5	90	10	180	20	0-5k
Total TDS	0		20k		50k		100k		200k		

Methodology

Introduction

The experiment was broken up into two separate parts. First, rheologic testing using a rheometer looking at properties of each FR fluid model. Each model will help in determining how to calculate the non-Newtonian Reynolds number for the specific fluid to get an accurate measurement of performance outside of the properties of this specific flow loop testing facility.

The outdoor flow loop at New Mexico Tech's Hydraulic Testing Facility uses a large motor and batches of fluid to test fluids performance under turbulent flow that will achieve high Reynold's numbers required for study of high rate flow through 1.5inch pipe. Both experiments were prepared with the same procedure and test matrix but on different scales. Common loadings for FR range from 0.25 to 1 gallon of FR per one thousand gallons of water (gpt). This range is converted to pounds per thousand gallons of water (pptg) for ease of measuring and is equivalent to 2 to 8.5 pptg. **Table 2** shows the test matrix used in the experiments. For the suspended solids tests calcium carbonate ($CaCO_3$) was used as a fine solid that would not dissolve in solution. (Kaufman, 2008).

Rheological Testing

For rheological testing the set up uses a Chandler Automated 3530 viscometer testing batches of FR solution without and with the presence of TDS. The Chandler viscometer is a rotary viscometer using a r1/b1 rotor and bob at speeds of 10, 100, 200, 300, 600rpm to build a profile of the shear rates to shear stresses to determine the rheological behavior of each batch of FR fluid. **Fig. 2** shows the setup of the testing equipment used.

Fig. 2: Rheological setup and equipment

Rheological Test procedure as follows:

1. Clean all equipment to prevent contamination to experiments.
2. Prepare 500ml of distilled water for batch test a ½ sample of 1 liter
3. Reduce chemical requirements, all chemical measurements reduced by ½.
4. Weigh out and mix FR at desired concentration until homogenous solution is achieved without entraining bubbles.
5. Weigh out NaCl and $CaCl_2$ to be added to batch test.
6. Mix until homogeneous solution is achieved.
7. Heat sample with heater until temperature of 100 degree Fahrenheit is reached.
8. Record dial readings at 10 rpm, 100 rpm, 200 rpm, 300 rpm, 600 rpm.
9. Tests were repeated until consistency between results was achieved.

Hydraulic Testing Facility

The New Mexico Tech Hydraulic Testing Facility uses a flow loop. The facility is equipped with a 90 gallon mixing tank that supplies a centrifugal pump ran by a 100 horsepower motor through mostly galvanized 2 inch lines and a PVC 1.5 inch test section. The system is set up with 3 measuring instruments that are capable of measuring pressure inside the line, flow rate, temperature, and differential pressure. A diagram in **fig. 3** shows the layout with instruments. All equipment is controlled inside the operating center near the flow loop using LabVIEW. The pump is controlled using a proportional integrative derivative (PID) controller for a steady flow. The hydraulic testing facility is located on New Mexico Institute for Mining and Technology campus.

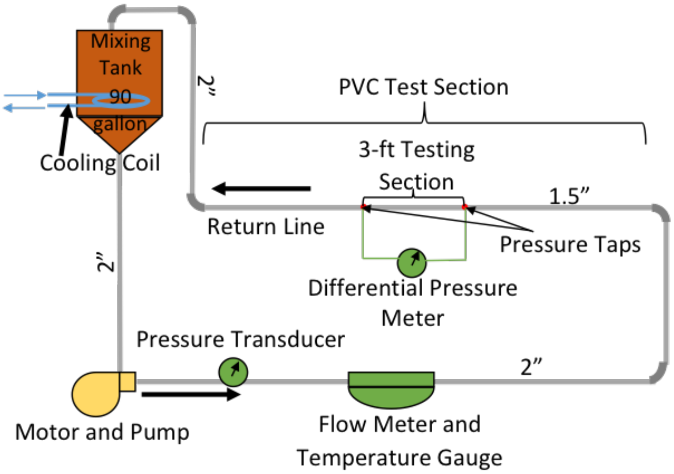

Fig. 3: Hydraulic Testing Facility Schematic

Hydraulic Testing Facility Procedure:

1. Clean all equipment to prevent contamination to experiments.
2. Prepare 90 gallons of tap water for batch test.
3. Adjust chemical concentrations to fit 90 gallon batches.
4. Heat water to 100 degrees Fahrenheit.

5. Weigh out and mix FR at desired concentration until homogenous solution is achieved at a water flow rate of 130 gallons per minute (gpm).
6. Weigh out NaCl and $CaCl_2$ at concentrations desired for batch test.
7. Mix until homogenous solution is achieved.
8. For the tests run with TSS ($CaCO_3$) are now added and allowed to spread throughout the loop.
9. Clear all air out of trapped areas in line through purge line on differential pressure meter.
10. Record readings at 10 gpm intervals from 40-160gpm.
11. Tests were repeated until consistency between results was seen.
12. After data collection up to 160 gpm flow line was cleaned out with fresh water and pump flow rate is set to 0 gpm.

Results and Discussion

Rheological Testing Without TDS

FR-A was subject to rheological testing at a range found in table 2. This profiled the FR solution as a shear thinning power law model fluid. Shear thinning meaning that as the shear rate increases, the apparent viscosity decreases. **Fig. 4** demonstrates this. This shear thinning ability of FR-A shows to be low comparatively to the other FRs used in this experiment. This first set of data without TDS in solution was the base case run on the FR. This allows for comparison on how these FRs model without any interference on their conventional friction reducing abilities. Notice from this plot that increasing the loading of FR shear thinning of the fluid goes down.

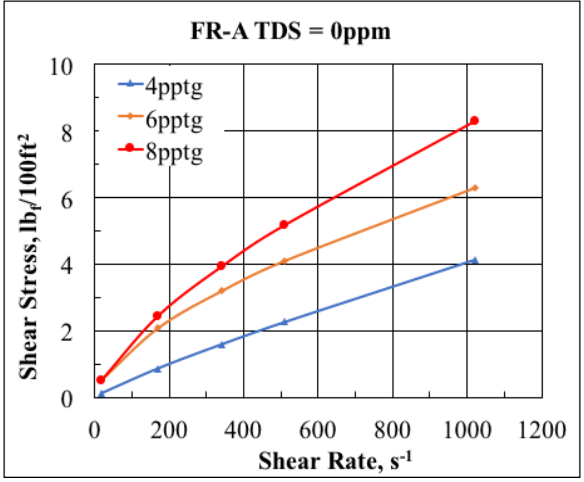

Fig. 4: FR-A TDS at 0ppm varying concentration of FR

The anionic FR-B indicated it has some of the best shear thinning capabilities of all FR's tested, having some of the lowest apparent viscosities measured. Reasons for this can be explained by design of this FR. It is designed to invert quickly in water meaning its polymer chain is smaller and does not create the apparent viscosity that the others do.

The cationic FR in the group, FR-C, showed that it's rheology fits between the other FRs shear thinning traits. This FR tends to react much like FR-A the main difference is its initial charge on the polymer.

Studying the friction reducers it is simple to notice that FR-A and FR-C have the most overall apparent viscosity when compared with FR-B. Wyatt et al., 2011 describes polymers in salt free solutions as having a strong Coulombic repulsions between like charges along the polymer backbone it stretchs and elongates individual chains. The polymers are surrounded by a cloud of counterions that exactly balances the charge on the chains so the solution maintains charge neutrality. This keeps the polymer chain complete in its original size and weight. The next section will introduce the TDS and how it effects the rheology of each FR.

Rheological Testing With TDS

When performing these tests, it was clear that apparent viscosity was decreasing after the addition of TDS to each fluid batch. **Fig. 5** shows FR-A at a concentration of 6-pptg without TDS on the left and on the right FR-A at the same concentration with TDS at a concentration of 50,000ppm. The sample on the left shows bubbles that were entrained into the fluid then left to sit. At the same time sample on the right was entrained with bubbles and allowed to rest. This is the visual showing bubbles are rising quicker to the surface when the sample has TDS mixed in solution, the apparent viscosity is much lower than that of the sample without TDS in solution, verifying the measured results. This also matches up closely with many others that have looked at PAM introduced to salt concentrations. Wyatt et al. (2011) mentioned how the addition of counter-ions, normally in the form of salt molecules, screens the electrostatic repulsions between charges along the backbone of the polymer chain. The screening of the electrostatic interactions allows the chain to fold up and assume a smaller more compact conformation. The degree to which a polymer molecule's conformation shrinks may be dependent on the stiffness of the polymer chain in solution. Since the molecular configuration changes, the solution rheology must also change. The addition of salt collapses polymer chains, leading to a large reduction in both viscosity and dynamic rheological properties. There is a high salt limit when the number of added salt ions is greater than the number of free counter-ions in solution. Y.B Lu et al. (2016) mentions while studying PAM in micro channel flow of non-Newtonian fluids concludes electrolytes (salts) have important effects on the flow of anionic and cationic PAM in aqueous solution. Salt ions can shield the electrostatic forces of polyanions and polycations effectively and shrink the volume of polyions. The small-volume polyinons correspond to a lower viscosity solution. Y. Lu et al. (2018) while looking at hydrophobically modified PAM containing crude oil emulsions explains that with the addition of salt the electrostatic repulsion dominates while the coiled molecular backbone also weakens the intermolecular association strength, causing the monotonical reduction of viscosity.

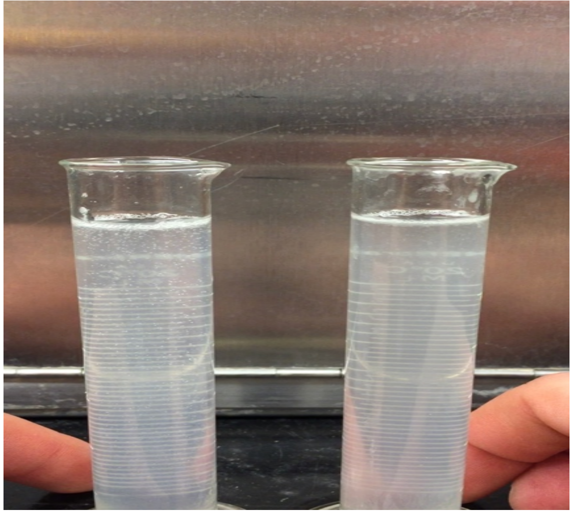

Fig. 5: 6pptg FR-A 0TDS on left and 50,000ppm TDS on right

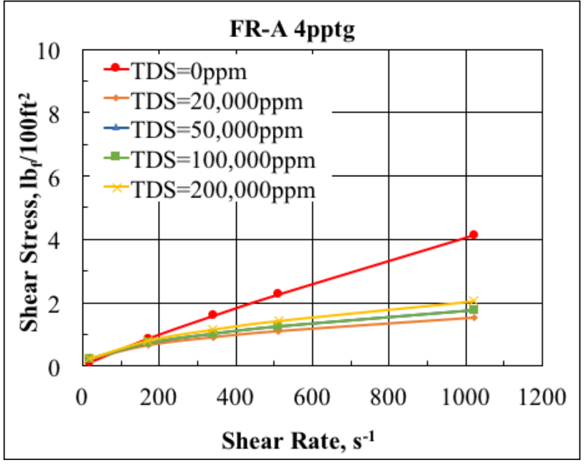

Fig. 6: FR-A at 4pptg varying concentration of TDS

Fig. 6 shows FR-As rheological test results without and with TDS at a concentration of 4pptg; it is also seen in this figure that once the TDS have mixed into solution the overall apparent viscosity has significantly dropped. Increasing the amount of the TDS in solution passed the initial 20,000ppm there is marginal change to the fluids rheology.

FR-Bs rheology after TDS have been introduced into solution it is unaffected by TDS at 4pptg. Increasing the loading concentration of FR-B and the TDS after 4pptg there is only minor changes in the rheology. When comparing these changes to the other FRs used FR-B is the least effected by TDS in solution. This shows to validate Wyatt et al. (2011) work where the high salt limit has been reached and no further free counterions are in solution. For the reason that this FR has been modified to work well in high saline conditions.

FR-Cs rheological tests are also greatly affected by the addition of TDS mixed in solution with it. The apparent viscosity of FR-C much like FR-A is reduced by the addition of TDS.

Correlations for Rheological Testing

Correlations were put together for each FR tested. The purpose, being able to know all of the possible iterations of rheological power law components base around the concentration of FR (C_{FR}), sodium chloride (C_{NaCl}), and calcium chloride (C_{CaCl2}). There are correlations for each FR and separated into two. One correlation without TDS and the other incorporating the addition of salts into the fluid. These models are pertinent only for predictions between the FR concentrations of 4 and 8pptg. **Eq. 1** and **eq. 2** show an example of the correlations for TDS calculation of FR-A. For the concentrations of TDS, the models are good between 0 and 200,000ppm TDS incorporating NaCl and $CaCl_2$. These models would also be able to fit into other PAMs that would match closely to the descriptions of these specific FRs.

$$n = \left[\left(-1.44\times10^{-5} \times C_{NaCl} - 1.61\times10^{-5} \times C_{CaCl_2} + 4.79\times10^{-3}\right) C_{FR} + 2.27\times10^{-4}\times C_{NaCl} + 2.56\times10^{-4}\times C_{CaCl_2} + 4.68\times10^{-1}\right] \quad (1)$$

$$K = 0.0571 \quad (2)$$

Fig. 7 show examples of the correlations fit to the experimental data gathered of FR-As 4pptg correlation without and with TDS against the recorded experimental data. Rheological data gathered from a conventional rotational viscometer should not be used to predict the actual performance of FR solutions under the actual slickwater fracturing pumping conditions. The main reasons are the very low Re (low shear rate) and the laminar flow in the gap between the bob and rotor sleeve of the viscometer leads to a minimum effect on the turbulent drag reduction.

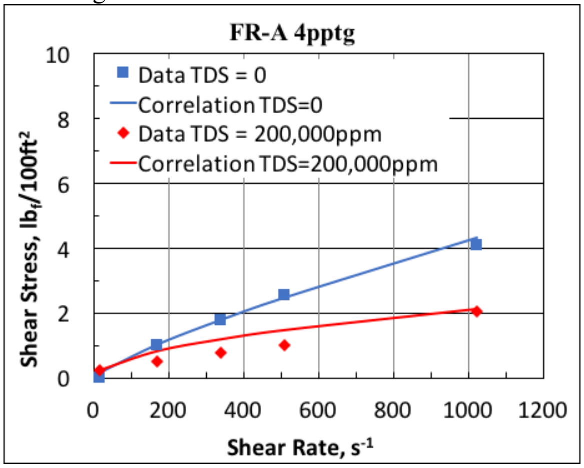

Fig. 7: Recorded experimental data alongside correlation

Hydraulic Testing Facility

An experimental execution for the tests ran on FR-A can be seen in **fig. 8** presenting test results of 4pptg concentration of FR-A with %FR as a function of the generalized Reynolds number without and with TDS. This allows for direct comparison of what is already known about the FR under its normal operating conditions and to compare this performance with TDS in solution batches. From figure 8 the maximum friction reduction that is achieved by FR-A without TDS at a Reynolds number just under 400,000 is about 65%. As the concentration of FR-A increases the amount of %FR goes down dramatically, so much so that at 8pptg concentration there is no positive %FR when TDS are not present. When TDS are present in solution the %FR is higher. In Fig. 8 it can be shown that the %FR that same Reynolds number is at 85% almost 20% increase. This percent increase could be explained by the folding of the polymer backbone, decreasing the viscosity, and allowing the friction reducing components of the PAM to contribute more, while the viscosity inhibits less of the friction reduction. It is clear to see that the test was able to see much higher %FR. This was not able to be directly compared to the solutions without TDS, we are not able to be certain of the exact performance, and a higher performance system would be required.

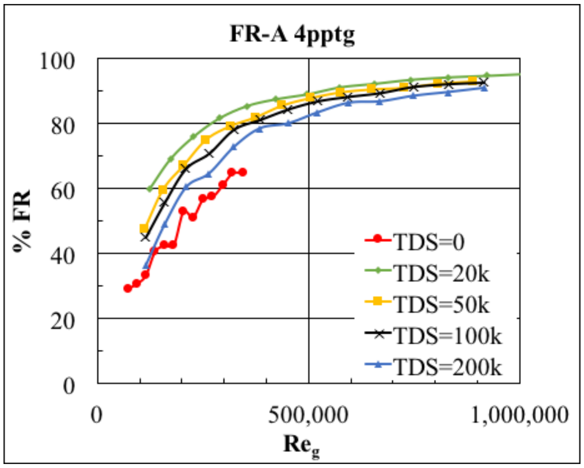

Fig. 8: FR-A 4pptg varying concentration of TDS as well as no TDS

Fig. 9 shows experimental points collected of FR-A at concentrations 4 to 8pptg at 20,000ppm TDS. This is one example of a trend that is clear to see as increasing the loading of FR does not contribute increase the %FR. This is also evident in the batches without TDS.

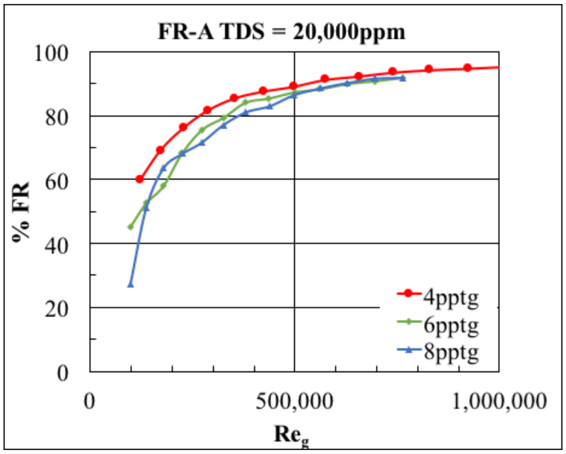

Fig. 10: Comparison of increased FR loading at TDS of 20,000ppm

FR-B is the other anionic FR tested under the same conditions FR-A. This FR is tailored to be the least effected by salts, this could be easily explained by the make-up of the FR. The backbone of this PAM has already been folded and reached a compact conformation. Meaning it no longer is effected by the addition of counterions; being that all the free counterions are occupied or blocked off. FR-B at 4pptg without TDS has its highest %FR at 700k Reynolds number with 90%. With TDS in solution this FR shows only a 5% drop at 700k Reynolds number at 85% friction reduction. It is also the only FR tested that lost performance in the tested Reynolds number range. This FR follows a trend of: when TDS concentration increases, the perfomance decreases, due to its initial design. **Fig. 10** exemplifies this. Increasing FR loading adversely effects this FRs performance as well, seen in **Fig. 11**.

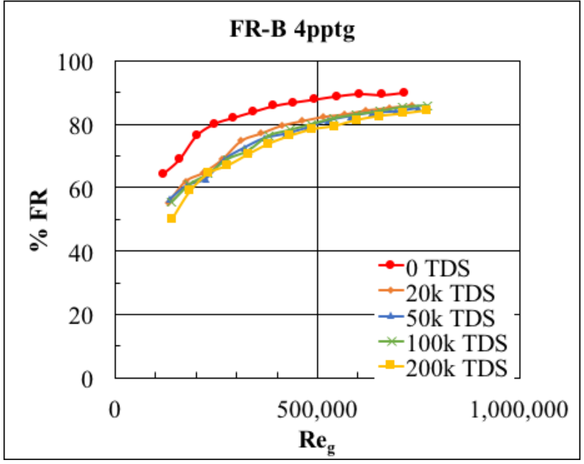

Fig. 10: FR-B at 4pptg and varying of TDS

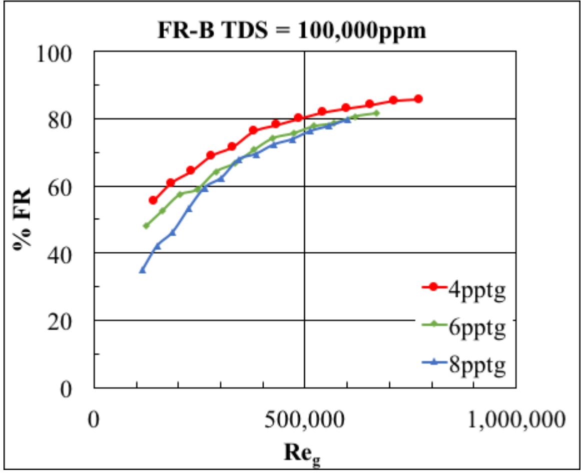

Fig. 11: Comparison of increased FR loading at TDS of 100,000ppm

The last FR tested is FR-C the cationic PAM of the group. From **fig. 12** it is possible to view that without TDS in solution the %FR is at 45-50% and with TDS in solution the %FR jumps up to 75% at 350,000 Reynolds number. This 25% increase is the largest increase in %FR comparatively between all three FRs after the TDS have been introduced. FR-C also follows the same trend as FR-A and FR-B; when FR loading is increased the overall performance of the FR goes down.

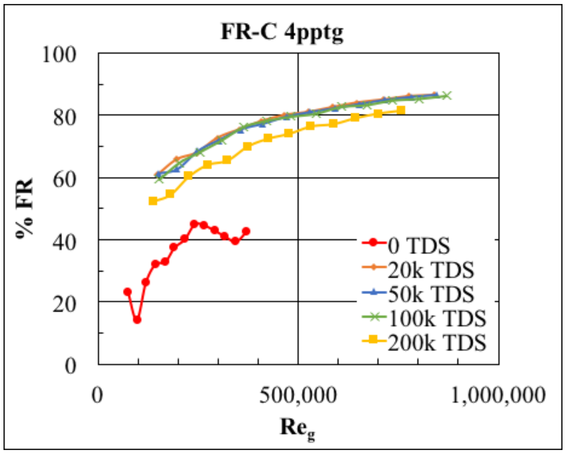

Fig. 12: FR-C at 4pptg varying TDS

The 4pptg concentration is the best performing concentration between the Reynolds numbers of 0 and 300,000 despite which FR is being used or if TDS are in solution. To get a clear idea of which FR would perform the best under these conditions plotting them all on the same plots will be shown in **fig. 13** and **fig. 14**. Fig. 13 clearly states which FR performs the best at 4pptg. The best performing FR at 4pptg and 0ppm TDS between the Reynolds numbers of 0 and 350,000 is FR-B. It gives the most %FR at about 85%. Next FR-A and FR-C give the performance at about 60% and 40% friction reduction respectively. The most significant results out of all of the plots is the amount of increased %FR over all of the FR after the introduction of TDS to each sample; fig. 14 looks at this more. After the salt is added in solution FR-A's and FR-C's viscosity is majorly decreased by shrinking the PAM molecule. This allows the friction reducing properties of the PAM to become more dominate and reduces the effect of the viscosity on friction reduction. Giving FR-A the most %FR at every concentration of TDS around 90% at 400,000 Reynolds number. This leaves FR-B and FR-C closely trailing behind anywhere from 5-10% less %FR.

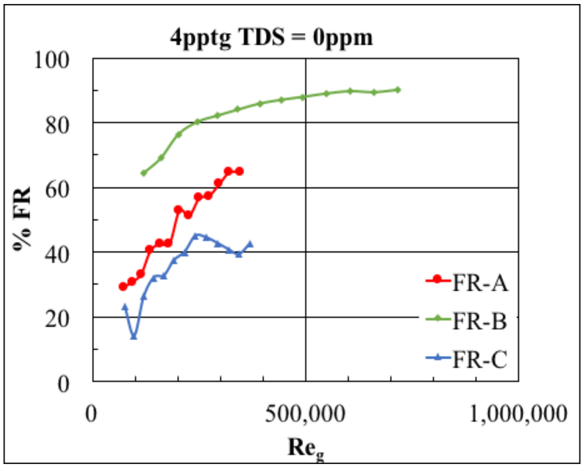

Fig. 13: 4pptg varying FR without TDS

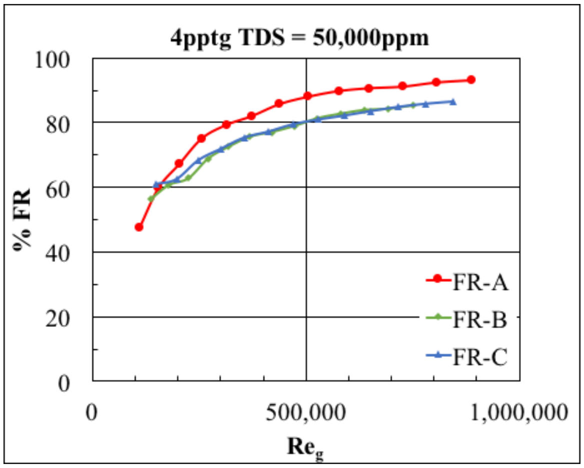

Fig.14: 4pptg varying FR with 50,000ppm TDS

At the hydraulic testing facility TSS tests were also performed. These test were run without and with TDS in solution to see how it affected the performance of each FR. FRs are a known flocculent and have been used for this attribute, this study observes if it takes away from the friction reduction component of PAM. Since $CaCO_3$ does not directly affect the rheology of the fluid and it is not soluble in water, it stays suspended in solution functioning much like the those found FB. Testing of the TSS took fewer experiments to grasp what was occuring to the fluids. The test matrix was reduced to run the high and low FR concentrations for each FR-A and FR-C at 4 and 8pptg. The TDS with TSS testing was also reduced and only incorporates 50,000ppm TDS for the reason it quickly showed a pattern. Tests were performed using one anionic FR (FR-A) and one cationic (FR-C). Each test followed the same procedure outlined for testing TDS with one addition, step 8.

Fig. 15 shows the testing results for the TSS testing completed on FR-A for a without and with comparison. This plot shows what was predicted about the FR being a flocculent and reacting with the TSS then proceeding to degrade the friction reduction component. Note that the actual degradation occurring is only 5% from original performance and the increase in the amount of TSS did not further degrade the performance within the TSS range of 100 to 5000ppm.

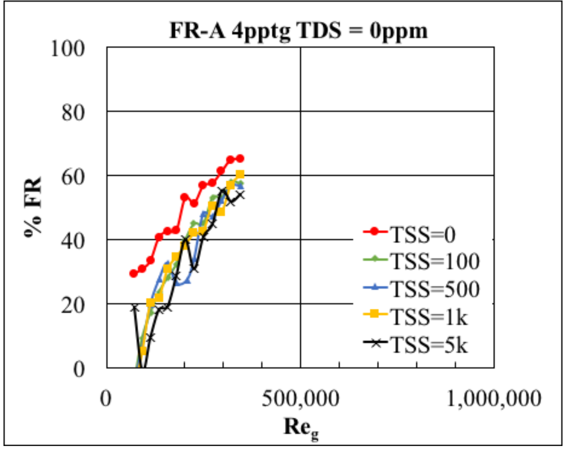

Fig.15: 4pptg with TDS at 0ppm and varying TSS

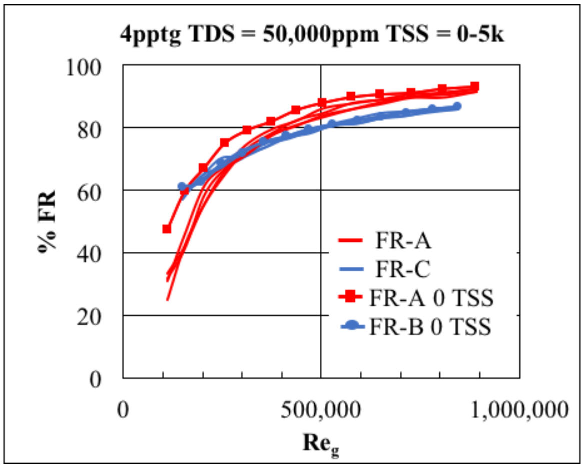

Fig.16: Comparison plot of 4pptg FR-A and FR-C at 50,000ppm TDS and TSS varying from 0-5kppm

In **fig. 16** the combined effects of TDS and TSS affected FR-A and FR-C batch at 4pptg and 50,000ppm TDS with varying concentrations of TSS. When the TDS are in solution the fluid is unaffected by the TSS. This means that when the salts have been added to the solution it takes away the fluids flocculating ability while not degrading the friction reduction component. It is also clear to see from this plot that the performance of FR-C is less than that of FR-A by a small range of 2 to 5%.

Testing 8pptg FR and 0 TDS varying concentration in TSS had no positive %FR per the findings in the previous tests done with 8pptg FR-A and FR-C. When TDS were introduced however it showed similar results to what was found in fig. 17 the increase in FR concentration had no unforeseen outcomes.

In summary, these solid suspension plots show that FR is definitely affected by the TSS when there is no TDS in solution. Once TDS have been introduced into the batch and TSS are then added it has relatively little effect on the performance on the friction reduction ability of the PAM. The TDS take away the flocculating component of the FR and then TSS have minimal effects on the overall %FR.

Conclusions and Future Work

This paper focuses on experimentally investigating the effects of salinity on the performance of FRs to optimize the reuse of the FB. Rheological and hydraulic tests were carried out for three commercial FRs at different concentrations. In addition, sodium chloride (NaCl), calcium chloride ($CaCl_2$), and TSS were added to the solution to study how the salinity (TDS) and suspended solids (TSS) affects the FR performance. The following conclusions can be drawn from the presented work.

- Rheological data obtained confirms that PAM in the presence of salt reduces the viscosity of the solution due to the bending of the polymer backbone and becoming a more compact conformation molecule effectively shrinking the number of polyanions in solution.

- Anionic FR-B performs better than anionic FR-A and cationic FR-C in fresh water. The %FR of FR-B at 4 pptg in fresh water is about 85% at 300,000 Reynolds number. FR-A and FR-C performs at 65% and 40% respectively under the same conditions. Increasing concentration of these FRs does not offer an increase in %FR. In addition, the performance of FR-B is less sensitive to salts than that of FR-A and FR-C by design.

- FR-A at 4pptg after being hydrated and TDS is introduced, studying the Reynolds numbers between 0 and 300,000 the %FR is higher than the performance of FR-A without TDS. The performance shows %FR at 85% almost 20% increase without TDS. This increase could be explained by the folding of the polymer backbone decreasing the viscosity allowing the friction reducing components of the PAM to contribute more while the viscosity inhibits less of the friction reduction. Based on knowing this conclusion it is highly recommended that this FR be used hydrated fresh in water, and cut with directly with flowback water during stimulation jobs.

- When TSS are added to solution of PAM the known effects of flocculation take away from the friction reducing properties. Once TDS have been introduced to the 4pptg FR-A solution and then TSS are added, the apparent viscosity and rheology have been altered, the flocculation component no longer has an impact on the friction reduction of the fluid. This is due to the fact that a fluid's flocculation abilities are a direct influence of the fluids rheology and its viscosity. Leaving TSS in FB water would not adversly affect the performance of anionic FR-A and cationic FR-C and recommend to be directly cut with hydrated PAM of similar descriptions.

These conclusions can be directly applied to any operator or service company using a PAM for stimulation, the recommendation is to take prehydrated PAM in fresh water and add a cut of flowback water directly and observe friction reduction inside the pipe go down requiring less horsepower on site and reusing flowback water without treatment of disposing TDS or TSS.

Acknowledgments

The authors thank Chemplex Solvay Group for providing all the materials used in this project as well as their financial and technical support throughout this study.

Nomenclature

$A_{cross\ sectional}$ = *Cross sectional area*
$CaCl_2$ = *Calcium Chloride*
C_{CaCl2} = *Concentration of* $CaCl_2$
C_{NaCl} = *Concentration of NaCl*
C_{FR} = *Concentration of friction reducer*
d = *Pipe diameter*

EPA = *Environmental Protection Agency*
f = *Fanning friction factor*
FB = *Flowback*
FR = *Friction Reducer*
g/L = *Gram per liter*
gpm = *Gallons per minute*
gpt = *Gallons per thousand gallons of water*
HTF = *Hydraulic testing facility*
inH_2O = *Inches of water*
K = *Consistency index*
lb_f = *Pounds force*
ml = *Milliliters*
n = *Flow behavior index*
NaCl = *Sodium Chloride*
PAM = *Polyacrylamide*
ppm = *Parts per million*
pptg = *Pounds per thousand gallons of water*
PID = *Proportional integrative derivative*
q = *Flow rate*
Re = *Reynolds number for Newtonian fluids*
rpm = *Rotations per minute*
Re_g = *Generalized Reynolds number*
SW = *Slickwater*
TDS = *Total dissolved solid*
v = *Fluid velocity*
%FR = *Percent friction reduction, %*
$\Delta P/\Delta l$ = *Pressure drop gradient, psi/ft*
ρ = *Fluid density*
γ_w = *Newtonian wall shear rate,* sec^{-1}

References

1. Barnes, Christopher M., et al. "The new reality of hydraulic fracturing: treating produced water is cheaper than using fresh." *SPE Annual Technical Conference and Exhibition*. Society of Petroleum Engineers - 174956, 2015.
2. Bourgoyne, A., Chenevert, M., Millheim, K., Young, F., “Applied Drilling Engineering” SPE Textbook Series, Vol. 2, Richardson, TX - Society of Petroleum Engineers – 1986.
3. Diamond, P., Harvey, J., Katz, J., Nelson, D., Steinhardt, P., “Drag Reduction by Polymer Addtives” JASON The MITRE Corporation – JSR-89-720 – October 1992
4. Kaufman, Phillip B., Glenn S. Penny, and Javad Paktinat. "Critical evaluation of additives used in shale slickwater fracs." SPE Shale Gas Production Conference. Society of Petroleum Engineers - 119900, 2008.
5. King, G. 2012 "Hydraulic Fracturing 101: What Every Representative, Environmentalist, Regulator, Reporter, Investor, University Researcher, Neighbor and Engineer Should Know About Estimating Frac Risk and Improving Frac Performance in Unconventional Gas and Oil Wells." Presented at the SPE Hydraulic Fracturing Technology Conference Held in The Woodlands, TX Feb. 2012.
6. Landahl, M. T. “Dynamics of Boundary Layer Turbulence and The Mechanism of Drag Reduction” Phys. Fluids 20 (1977) S55.
7. Lu, Yao, et al. “Salt Effect on Hydrophobically Modified Polyacrylamide-Containing Crude Oil Emulsions: Stability and Rheology Study.” Colloid and Polymer Science, vol. 296, no. 3, 2018, pp. 515–527.
8. Lu, Y.B, et al. “Experimental Study of Microchannel Flow for Non-Newtonian Fluid in the Presence of Salt.” Experimental Thermal and Fluid Science, vol. 74, 2016, pp. 91–99.
9. Lumley, J. L. “Drag Reduction in Turbulent Flow by Polymer Additives.” Journal of Polymer Science: Macromolecular Reviews, vol. 7, no. 1, 1973, pp. 263–290.
10. Mantell, M. “Produced Water Reuse and Recycling Challenges and Opportunities Across Major Shale Plays” EPA Hydraulic Fracturing Study Technical Workshop #4, 2011
12. Nguyen, T. C., Romero, B., Vinson, E., & Wiggins, H. “Effect of salt on the performance of drag reducers in slickwater fracturing fluids. Journal of Petroleum Science and Engineering”. 2017
13. Oraki Kohshour, Iman, et al. "Examination of Water Management Challenges and Solutions in Shale Resource Development-Could Waterless Fracturing Technologies Work?" *Unconventional Resources Technology Conference*. Unconventional Resources Technology Conference, 2016.
14. Paktinat, Javad, et al. "High brine tolerant polymer improves the performance of slickwater frac in shale reservoirs." *North American Unconventional Gas Conference and Exhibition*. Society of Petroleum Engineers - 144210, 2011.
15. U.S. EPA. Hydraulic Fracturing for Oil and Gas: “Impacts from the Hydraulic Fracturing Water Cycle on Drinking Water Resources in the United States (Final Report)”. U.S. Environmental Protection Agency, Washington, DC, EPA/600/R-16/236F, 2016.
16. Virk, P. S. “Drag Reduction Fundamentals.” Aiche Journal, vol. 21, no. 4, 1975, pp. 625–656.
17. Wyatt, Nicholas B., Casey M. Gunther, and Matthew W. Liberatore. "Increasing viscosity in entangled polyelectrolyte solutions by the addition of salt." Polymer 52.11 (2011):2437-2444.

Appendix A

Comerrcial FRs Discriptions

Three commercial FRs are used in the experiment: anionic Friction Reducer A (FR-A), anionic Friction Reducer B (FR-B), and cationic Friction Reducer C (FR-C). FR-A and FR-B are anionic polymers and FR-C is cationic polymer. Below is the detailed description of each polymer.

Anionic FR-A contains anionic acrylamide copolymers and surfactants in a mineral oil base with a density of 1068 kg/m^3 (8.92 ppg). It is compatible with moderate concentrations of salts and with anionic or nonionic surfactants. It hydrates rapidly, even in cold water, to give optimal performance. It is claimed to be an economical, extremely efficient anionic friction reducer designed for use in freshwater and light brines with TDS less than 25000 ppm.

Anionic FR-B contains anionic acrylamide copolymers and surfactants in a mineral oil base with a density of 1089 kg/m^3 (9.09 ppg). It is compatible with moderate concentrations of salts and with anionic or nonionic surfactants. It is believed to give an extremely efficient anionic FR for oilfield brines or for freshwater. FR-B is recommended for use with fluids with TDS less than 150000 ppm.

Cationic FR-C contains cationic acrylate polymers and surfactants in a mineral oil base with a density of 1059 kg/m^3

(8.84 ppg). It is designed to be compatible with typical acid inhibitors and with cationic or nonionic nonemulsifiers. It is an easily-handled, highly efficient friction reducer for freshwater, brines, and acids.

Calculation of Friction Reduction

Laminar calculations used while analyzing the rheology of each FR while using the Chandler viscometer. The raw data consists of dial readings from the Chandler as well as rotations per minute (rpm). Each fluid batch has five speeds and five dial reading recordings. Each readingis converted to shear stress ($\frac{lbf}{100ft^2}$) and shear rate(s^{-1}). To observe and understand each set of fluid batches they were plot then fit with a power law regression. The power law properties of flow behavior index (*n*) and consistency index (*K*) were acquired to further study the fluid in turbulent conditions through the Reynolds number.

While analyzing friction reduction properties a few equations are required to understand how the fluid is working. The measurements gathered with the flow loop and the rheology testing are utilized express the Reynolds number that will be used to compare to %FR. Flow rate is converted from gpm to average velocity through **eq. 4**. In order to get the average velocity an inside diameter of the test section is required for the cross sectional area. For these experiments the test section has an inside diameter of 1.6 inches.

$$\bar{v} = \frac{q}{A_{cross\ sectional}} \tag{4}$$

The measured pressure drop inside the pipe is recorded through the differential pressure meter over a 3ft section recorded in inches of water (inH$_2$O). The inH$_2$O is converted to pounds per square inches per foot (psi/ft). Next finding the fanning friction factor inside of the pipe for each pressure drop measurement the equation from Bourgoyne, 2015 [2] **eq. 5** is used.

$$f = \frac{25.8\frac{\Delta p}{\Delta L}d}{\rho \bar{v}^2} \tag{5}$$

This eq.5 is derived from the definition of the friction factor. It has also been converted to field units. This equation will be used for finding the Reynolds numbers of each fluid tested. It is independent of fluid rheology.

Before testing with SW batches a baseline test was run with tap water. This baseline was analyzed with **eq. 6** shows the field unit equation used for water in this experiment to acquire the Reynolds number for a Newtonian fluid under turbulent flow conditions.

$$N_{Re} = \frac{928\rho\bar{v}d}{\mu} \tag{6}$$

The next equation was developed by Dodge and Metzner the correlation uses the apparent viscosity inside the Reynolds number criterion under Newtonian conditions. **Eq. 7** is in the field unit form from Bourgoyne, 2015 [3].

$$N_{Re_g} = \frac{89{,}000\rho\bar{v}^{2-n}}{K}\left(\frac{0.0416d}{3+\frac{1}{n}}\right)^n \tag{7}$$

To compare the SW batches an equation is required that compares the friction reduction at comparable Reynolds numbers with that of water. Which is completed with %FR of the fanning friction factor found in **eq. 8**. This equations derivation can be found in T. Nguyn et. al., 2016 [12].

$$\%FR = \frac{f_w - f_{FR}}{f_w}\times 10 \tag{8}$$

Correlations for Rehological Properties

FR-A correlation without TDS is seen in **eq. 9** the flow behavior index (n) and **eq. 10** the consistency index (K).

$$n = -0.0355C_{FR} + 0.9441 \tag{9}$$

$$K = 0.0179C_{FR} - 0.055 \tag{10}$$

The saline correlation for FR-A can be seen in **eq. 11** and **eq. 12** the flow behavior index and consistency index consecutively.

$$n = \left[\left(-1.44\times10^{-5}\times C_{NaCl} - 1.61\times10^{-5}\times C_{CaCl_2} + 4.79\times10^{-3}\right)C_{FR} + 2.27\times10^{-4}\times C_{NaCl} + 2.56\times10^{-4}\times C_{CaCl_2} + 4.68\times10^{-1}\right] \tag{11}$$

$$K = 0.0571 \tag{12}$$

FR-Bs correlation without TDS is expressed in **eq. 13** for *n* and **eq. 14** showing *K*.

$$n = 0.0145C_{FR} + 0.663 \tag{13}$$

$$K = 0.015 \tag{14}$$

The correlation for FR-B containing TDS concentrations of NaCl and CaCl$_2$ seen in **eq. 15** for *n* and **eq. 16** for *K*.

$$n = \left[\left(1.24\times10^{-5}\times C_{NaCl} + 1.39\times10^{-5}\times C_{CaCl_2} + 6.71\times10^{-3}\right)C_{FR} - 1.17\times10^{-5}\times C_{NaCl} + 1.33\times10^{-5}\times C_{CaCl_2} + 7.36\times10^{-1}\right] \tag{15}$$

$$K = 0.01 \tag{16}$$

FR-C Model predictions without TDS concentrations can be seen in **eq. 17** for *n* and **eq. 18** for *K*.

$$n = -0.0318C_{FR} + 0.9674 \tag{17}$$

$$K = 0.009C_{FR} + 0.0276 \tag{18}$$

FR-Cs TDS model predictions can be seen in **eq. 19** for *n* and **eq. 20** for *K*.

$$n = \left[\left(-1.15\times10^{-5}\times C_{NaCl} - 1.24\times10^{-5}\times C_{CaCl_2} + 1.28\times10^{-2}\right)C_{FR} + 2.22\times10^{-4}\times C_{NaCl} + 2.5\times10^{-4}\times C_{CaCl_2} + 6.86\times10^{-1}\right] \tag{19}$$

$$K = 0.01 \tag{20}$$